JOURNAL OF SPACECRAFT AND ROCKETS
Vol. 36, No. 5, September–October 1999

Model-Based Thruster Leakage Monitor for the Cassini Spacecraft

Allan Y. Lee*
Jet Propulsion Laboratory, California Institute of Technology, Pasadena, California 91109-8099

The Cassini spacecraft uses thrusters to perform many spacecraft control functions: to detumble the spacecraft, to maintain three-axis attitude control, to perform small trajectory correction burns, to desaturate the reaction wheels, and others. If one of the prime thrusters leaks, e.g., becomes stuck open, the opposing thrusters will be fired extra hard to maintain the commanded spacecraft pointing attitude. Obviously, the resultant draining of hydrazine and the excessive firings of thrusters cannot be allowed to persist indefinitely. A set of three model-based thruster leakage detection monitors has been designed, tested, and implemented in the flight software to protect Cassini against the occurrence of this highly unlikely event. Test results indicated that these monitors can detect thruster leaks of all sizes quickly and robustly. Once the leak is detected, the onboard fault protection logic will activate corrective actions, including the swapping of thruster branches.

Nomenclature

$\boldsymbol{H}_{\text{rwa}}$ = angular momentum vector of reaction wheels, Nms
I = spacecraft inertia tensor, kg-m^2
$\boldsymbol{R}$ = residual angular momentum vector, Nms
R_k^{corr} = correction term for the k component of $\boldsymbol{R}$, where k is equal to x, y, and z, Nms
R_T = angular momentum threshold, Nms
$\boldsymbol{T}_{\text{env}}$ = torque on spacecraft due to gravity gradient, Nm
$\boldsymbol{T}_{\text{leak}}$ = torque on spacecraft due to a leaky thruster, Nm
T^{limit} = preselected time threshold, s
$\boldsymbol{T}_{\text{pms}}$ = torque on spacecraft due to propulsion system, Nm
$\boldsymbol{T}_{\text{rwa}}$ = torque on spacecraft due to reaction wheels, Nm
T_k^{trigger} = time it takes $|R_k|$ to exceed R_T, where k is equal to x, y, and z axes, s
Y_j = jth Y-facing thruster, where j is equal to 1–4
Z_j = jth Z-facing thruster, where j is equal to 1–4
ΔV = spacecraft velocity vector change, m/s
$\boldsymbol{\epsilon}$ = residual torque vector, Nm
$\boldsymbol{\eta}$ = thruster to thruster uncertainty
$\boldsymbol{\omega}$ = spacecraft angular velocity vector, rad/s
$\dot{\boldsymbol{\omega}}$ = spacecraft angular acceleration vector, rad/s^2

Introduction

REACTION control thrusters are used by spacecraft to perform many functions: to maintain three-axis attitude control, to perform small trajectory correction burns, and others. For redundancy, the prime set of thrusters is usually backed up by a second set. If one of the prime thrusters fails, e.g., becomes stuck open or stuck closed, the expulsing hydrazine will begin to impart angular momenta on the spacecraft. Obviously, the draining of hydrazine, the excessive firings of opposing thrusters, and the accumulation of angular momentum on the spacecraft cannot be allowed to persist indefinitely. To protect the Cassini spacecraft (which was launched recently) against the occurrence of a leaky thruster (an unlikely event), a set of three leak detection monitors has been designed, tested, and implemented in the flight software. This error monitor design takes advantage of the fact that the dynamical motion of the spacecraft is being governed by Euler's equation. The occurrence of a leaky thruster will impart torque on the spacecraft, which will upset the nominal Euler's equation. The monitoring of angular momenta that are generated by torque from a leaky thruster is one effective way to detect the presence of a leaky thruster. Once a leak is detected, the onboard fault protection logic will activate autonomous corrective actions, including the swapping of thruster branches.

Received 5 October 1998; revision received 19 January 1999; accepted for publication 19 January 1999.

*Senior Member, Technical Staff, Mail Stop 198-235, Avionic Systems Engineering Section, 4800 Oak Grove Drive.

Cassini and Its Mission

The Cassini spacecraft (S/C) was launched on 15 October 1997 by a Titan 4B launch vehicle. After an interplanetary cruise of almost seven years, it will arrive at Saturn in July 2004. To save propellant, Cassini will make several gravity-assist flybys: two at Venus and one each at Earth and Jupiter. Figure 1 shows the interplanetary trajectory design of the Cassini spacecraft.

Unlike Voyagers 1 and 2, which only flew by Saturn, Cassini will orbit the planet for at least four years. Major science objectives of the Cassini mission include investigations of the configuration and dynamics of Saturn's magnetosphere, the structure and composition of the rings, the characterizations of several of Saturn's icy moons, and others. The Huygens probe, developed by the European Space Agency, will be released in September 2004 and will study the atmosphere of Titan, the only moon in the solar system with a substantial atmosphere. Detailed descriptions of various science instruments carried onboard the Cassini spacecraft are given in Ref. 1.

The Cassini spacecraft with its magnetometer boom deployed is shown in Fig. 2. The central structure of the S/C carries the propulsion module with tanks for both the monopropellant and bipropellant. It also supports the Huygens probe and the remote sensing pallet (on which various high-resolution imaging cameras are mounted). Above the central structure is the upper equipment module and the high-gain antenna (HGA). One of the two low-gain antennas is collocated and coboresighted with the HGA, whereas the second is mounted just underneath the probe. Below the central structure is the lower equipment module, which supports three radioisotope thermoelectric generators (power generators). Below the lower equipment module is a redundant set of two rocket engine assemblies. The lower equipment module also supports a structure on which are mounted four thruster pods.

At launch, the total mass of the S/C is 5573.8 kg, and its inertia tensor is [8782 −124 114; −124 9050 −50; 114 −50 3773] kg-m^2. The knowledge uncertainties of the mass and moments of inertia of the dry S/C are better than ±0.5% and ±10%, respectively, whereas the uncertainty of the products of inertias is better than ±75 kg-m^2. The knowledge uncertainty of the S/C's center of mass is better than ±5 cm. As monopropellant and bipropellant are being depleted over time due to thruster firings and main engine burns, there will be continuous changes in these S/C's inertia properties. Additionally, large changes in these inertia properties will occur at the following discrete events: deployment of the magnetometer boom, ejection of the Huygens probe, and after both the long Deep Space Maneuver

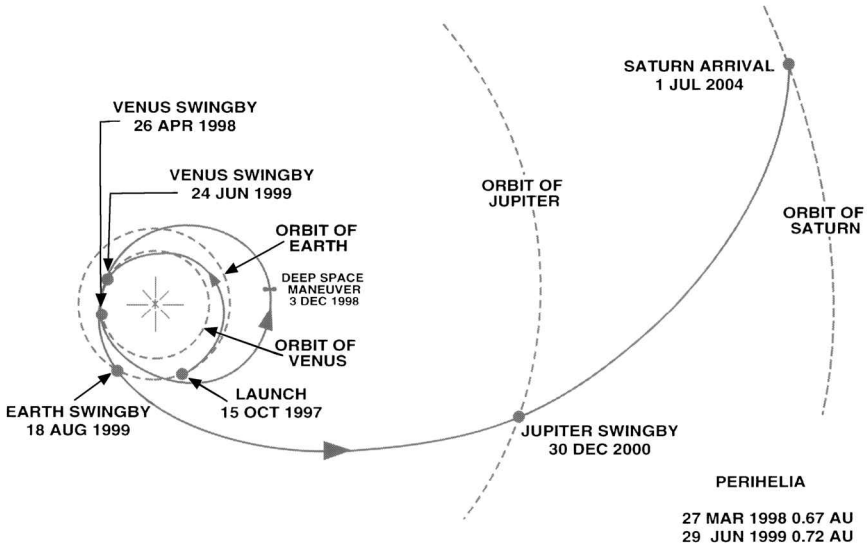

Fig. 1 Cassini interplanetary trajectory.

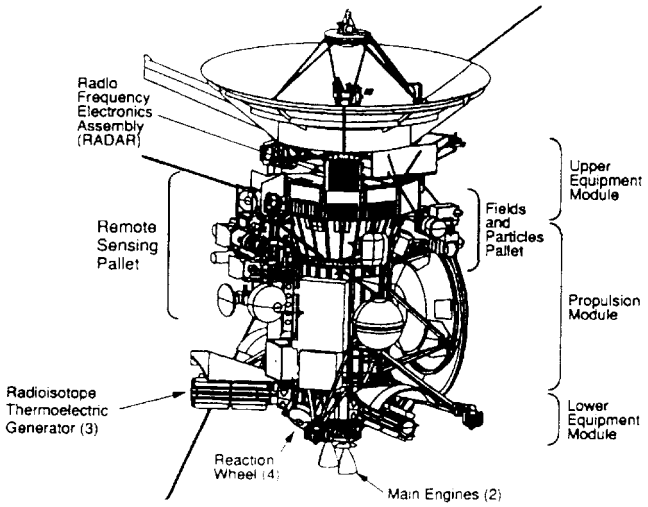

Fig. 2 Cassini spacecraft.

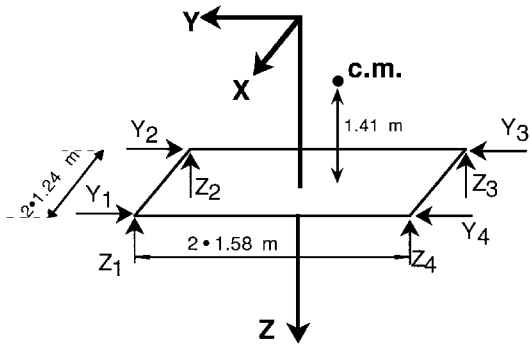

Fig. 3 Thruster pod locations.

and Saturn Orbit Injection burns. Uncertainties associated with our knowledge of these S/C inertia properties, as well as those of the thrusters, make the task of designing a thruster leakage detection scheme very challenging.

Thrusters and Their Functions

Cassini uses a set of eight thrusters to maintain three-axis attitude control of the spacecraft. Figure 3 shows the locations of the four thruster cluster pods.

Pointing controls about the S/C's X and Y axes are performed using four Z-facing thrusters. Controls about the Z axis are performed using four Y-facing thrusters. The eight thrusters on the A branch are being backed up by another set of eight thrusters on the B branch. In addition to performing the vital task of pointing control, thrusters also serve the following functions: to detumble the S/C and bring it to a quiescent state after the Centaur/Cassini and Huygens/Cassini separations, to perform a full-sky search to locate the sun, to slew the S/C about a selected axis, to periodically unload the angular momenta that are accumulated on the reaction wheel assemblies (RWAs), and to perform small trajectory correction maneuvers, which are sometimes called ΔV burns. Algorithms that perform these thruster-based S/C control functions are described in Ref. 2.

The monopropellant propulsion system for Cassini is of the blowdown type, with one planned recharge. With this system, the hydrazine tank pressure, which is $\approx$2550 kPa at launch, will decay slowly with time as hydrazine is being depleted due to thruster firings. The nominal thrust of these thrusters at launch is $\approx$1 N. Knowledge uncertainties of the thrust produced by these thrusters include a $\pm$7% pulse-to-pulse and a $\pm$5% thruster-to-thruster variation.[3] The angular misalignment between the actual thrust vector and the S/C axes is below 1 deg, and the locations of the thruster nozzle centers are known to be better than 1.1 cm (Ref. 3).

Leakage Detection Requirements

If one of the eight prime thrusters leaks, e.g., becomes stuck open, the expulsing hydrazine will impart angular momenta on two of the three S/C axes. In response to the resultant attitude control errors that appeared on the affected axes, appropriate thrusters will be fired to maintain the commanded spacecraft attitude. Obviously, the draining of hydrazine and the excessive firings of thrusters cannot be allowed to persist indefinitely. A set of three leak detection monitors (one for each S/C axis) has been designed, tested, and implemented in the flight software to protect Cassini against the occurrence of this highly unlikely event. Once a leak is detected, the onboard fault protection logic will activate autonomous corrective actions, including the swapping of thruster branches.

The main requirement on the thruster leakage detection monitor design is spelled out in Ref. 4:

> In the "Cruise", "Earth Approach", and "Venus/Earth Flybys" modes, the Attitude Control Subsystem shall be able to detect any single thruster leak that applies an average torque of at least 0.005, 0.001, and 0.05 Nm, respectively, about any S/C axis, and shall isolate that single thruster leak before it applies more than 100 Nms of angular momentum about any S/C axis.

In the cruise mode, Cassini Mission Operations will communicate with the S/C, at least once a week. Over this one-week time span, a

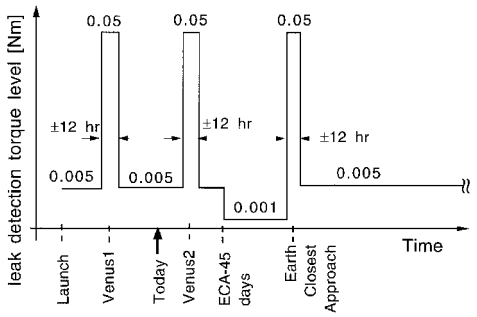

Fig. 4 Thruster leakage torque detection levels.

thruster leak that resulted in a disturbance torque of 0.005 Nm will drain not more than 1.15 kg of hydrazine. This amount of hydrazine represents only 0.8% of the total hydrazine load. During the Venus 1, Venus 2, and Earth flybys, gravity gradient torques exerted on the S/C axes are comparable with 0.005 Nm. Hence, the torque detection level is relaxed (increased) to 0.05 Nm. On the other hand, during the Earth approach phase of the mission, the S/C trajectory must be controlled very precisely. Therefore, the torque detection requirement is tightened (decreased) to 0.001 Nm. Figure 4 shows the variation of the thruster leakage torque detection requirement over the first two years of the Cassini mission.

Implicit in the stated requirement is the need to detect thruster leaks even while the S/C is in a nonquiescent state, e.g., during a spiral sun search maneuver. A thruster leakage detection error monitor design that meets this requirement will be described. However, if instead the requirement was to detect thruster leaks only when the S/C is in a quiescent state, then the approaches described in the Appendix, which are simpler, could do the same job.

Leak Detection Monitor Design

Conventional fault detection methods typically involve the monitoring of one or more of the following quantities: measured system output(s), estimated system state(s), and estimated process parameter(s).[5] These measured or estimated quantities are then compared with their normal values, and their deviations are computed. If any one of these deviations persistently exceeds its preselected allowable tolerance, an error monitor is triggered to report this abnormality.

This conventional error detection approach is not applicable here because there is not any single measured or estimated quantity that signals the presence of a leaky thruster. A different approach must be taken in designing the thruster leakage detection monitors. To this end, we first note that the rotational motion of the S/C is governed by the following Euler equation:

$$I\dot{\omega} + \omega \times (I\omega + \boldsymbol{H}_{\text{rwa}}) = \boldsymbol{T}_{\text{rwa}} + \boldsymbol{T}_{\text{pms}} + \boldsymbol{T}_{\text{env}} + \boldsymbol{T}_{\text{leak}} + \epsilon \quad (1)$$

In Eq. (1), I is the S/C inertia tensor. The S/C angular velocity vector ω is estimated by an onboard attitude estimator, but it is typically noisy. Hence, the commanded angular velocity vector generated by an onboard attitude commander is used instead. The S/C angular acceleration vector $\dot{\omega}$ is not estimated by the attitude estimator. Again, we use that generated by the attitude commander. The angular momentum vector of the three RWAs $\boldsymbol{H}_{\text{rwa}}$ is added to the S/C angular momentum $I\omega$ to generate the total S/C angular momentum vector.

Reaction torques exerted on the S/C by the RWAs, $\boldsymbol{T}_{\text{rwa}}$, are estimated onboard by an RWA manager (a flight software object). Torque exerted on the S/C due to thruster firings, $\boldsymbol{T}_{\text{pms}}$, is not available directly. Instead, an onboard propulsion manager estimates the force impulses due to all prime thruster firings. Using the estimated thruster moment arms, these force impulses are next converted into three per-axis torque impulses. In effect, what we have is $\int \boldsymbol{T}_{\text{pms}}\,\mathrm{d}t$. These estimated angular momentum impulses are typically noisy and contain errors due to uncertainties in our knowledge associated with both the thrusters and the S/C's c.m. location.

Environmental torques due to gravity gradient, solar radiation, magnetic field, atmospheric, etc., are captured in $\boldsymbol{T}_{\text{env}}$. These torques are typically very small except during planet and Titan flybys.

Table 1 Identity of the leaky thruster

Leaky thruster	Angular momentum rates, Nm		
	$\dot{R}_x$	$\dot{R}_y$	$\dot{R}_z$
Y_1	+	0^+	−
Y_2	+	0^+	+
Y_3	−	0^+	−
Y_4	−	0^+	+
Z_1	−	+	0^+
Z_2	−	−	0^+
Z_3	+	−	0^+
Z_4	+	+	0^+

Torque due to a leaky thruster is represented by $\boldsymbol{T}_{\text{leak}}$. For example, if the Z_1 thruster leaks, there will be a negative and a positive torque acting on the S/C's X and Y axes, respectively (but with no torque on the Z axis). Finally, ϵ is used in Eq. (1) to account for both the knowledge uncertainties associated with various S/C parameters, e.g., inertia tensor, and estimation errors associated with various derived S/C variables, e.g., angular momentum impulses.

Next, we note that various terms in the Euler equation are available onboard. This allows us to monitor the entire Euler equation instead of monitoring an individual measured/estimated quantity. Nominally, the Euler equation does not contain the $\boldsymbol{T}_{\text{leak}}$ term, and any deviation from this condition indicates a possible fault. Let us define the following residual angular momentum vector $\boldsymbol{R}$:

$$\boldsymbol{R}(t) = \int_0^t \{\boldsymbol{T}_{\text{leak}} + \epsilon\}\,\mathrm{d}\tau$$

$$= \int_0^t \left\{I\dot{\omega} + \omega \times (I\omega + \boldsymbol{H}_{\text{rwa}}) - \boldsymbol{T}_{\text{rwa}} - \boldsymbol{T}^f_{\text{pms}}\right\}\mathrm{d}\tau \quad (2)$$

where $\boldsymbol{T}^f_{\text{pms}}$ is a low-pass-filtered version of the noisy raw data, and $\boldsymbol{T}_{\text{env}}$ has been neglected in Eq. (2). With no leak, $\boldsymbol{R}$ contains only small zero-mean random fluctuations, due to ϵ. Whenever a leak appears, two of the three $\boldsymbol{T}_{\text{leak}}$ components will be nonzero. If the leak persists, the resultant nonzero components of $\boldsymbol{R}(t)$ will grow (either increase or decrease) with time. In time, one of these components will exceed a preselected angular momentum threshold (R_T): $|R_i| \geq R_T$ (where $i = x$, y, or z axis), triggering the error monitor for that particular S/C axis. Note also that the polarities of R_i ($i = x$, y, and z axis) reveal the identity of the leaky thruster. See Table 1 for a complete mapping between a leaky thruster and the polarities of the corresponding $\dot{R}_i$ ($i = x$, y, and z axis).

To detect a leak before it imparts more than 100 Nms on any S/C axis, we select R_T to be 50 Nms. The rationale for this selection is as follows. The first time the 50-Nms threshold is exceeded, a fault protection activation rule, in attempting to stop the leak, will reset the controller unit for the thruster valve drive electronics. At the same time, all three components of $\boldsymbol{R}$ are reset to zero. If the reset of the controller unit does not stop the leak, and if the leak persisted, the same two $\boldsymbol{R}$ components will again grow with time. The second time the 50-Nms threshold is exceeded, fault protection activation rules will initiate swapping of thruster branches, which will stop the leak. In this way, we will be able to stop the leak before it imparts a total of 100 Nms on any spacecraft axis. The selected 50-Nms angular momentum threshold is changeable via a command.

Coping with Uncertainties

Not all of the uncertainty terms that affect $\boldsymbol{R}$ are random in nature. In particular, the thruster-to-thruster variation can impart systematic errors to the Euler equation, causing $\boldsymbol{R}$ to grow with each thruster firing, even without a leak. As such, prolonged thruster firings could trigger the $|R_i| \geq R_T$ criterion. Two modifications are made to the described leak detection scheme to avoid such a false alarm.

First, a correction vector $\boldsymbol{R}^{\text{corr}}$ is estimated to account for angular momentum accumulation due to thruster-to-thruster variation. The estimation of the X-axis component of $\boldsymbol{R}^{\text{corr}}$ is given here as an illustration.

Rotations about the spacecraft X axis are made using either the Z_1 and Z_2 pair or the Z_3 and Z_4 pair. Hence, the X-axis component

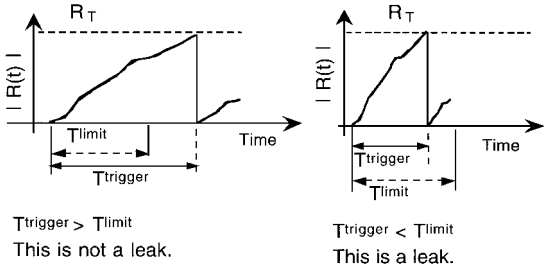

Fig. 5 Leak detection scheme.

of $\boldsymbol{R}^{\text{corr}}$ is proportional to both the differential thrusters' impulses and the size of the thruster-to-thruster uncertainty estimate:

$$\Delta J_x = \left|\Delta J_{Z_3} + \Delta J_{Z_4} - \Delta J_{Z_1} - \Delta J_{Z_2}\right| \tag{3}$$

$$R_X^{\text{corr}} = 2 \times \eta \times 1.6 \times \Delta J_X \tag{4}$$

where ΔJ_{Z_j} is the accumulated impulses due to the Z_j thruster over the last real time interrupt. These accumulated impulses are available from the onboard propulsion manager. The thruster-to-thruster uncertainty η is estimated to be 0.05, i.e., 5%, at launch. If a better estimate of η is available postlaunch, the current estimate could be updated using the same command that was used to alter R_T. The factor 1.6 represents the average magnitude of the four Z thrusters' moment arms (in meters). The factor 2 is used to account for the standard deviation of a variable that is the sum/difference of four variables, each with a standard deviation of σ, being 2σ. The Y and Z components of $\boldsymbol{R}^{\text{corr}}$ are estimated similarly. The correction vector $\boldsymbol{R}^{\text{corr}}$ is then added to $\boldsymbol{R}$, and the resultant modified $\boldsymbol{R}$ is used in the momentum threshold check.

Next, after the angular momentum threshold is exceeded, a second condition, $T_j^{\text{trigger}} \le T^{\text{limit}}$, is checked before any fault protection action is initiated. Here, T_j^{trigger} (j is the S/C axis whose $|R_j|$ exceeded the angular momentum threshold) is the time it takes $|R_j|$ to exceed R_T since it was last reset. The threshold T^{limit} is a time-domain threshold that is to be preselected. If T_j^{trigger} is larger than T^{limit}, then we conclude that the R_T threshold was exceeded not because of a thruster leak but is rather due to the systematic accumulation of angular momentum from prolonged thruster firings. On the other hand, if T_j^{trigger} is smaller than T^{limit}, then there is a real leak, and corrective action from the onboard fault protection logic is needed. This time-domain trigger criterion is shown in Fig. 5.

For the cruise mode, we select T^{limit} to be 10 h. Note that this value is larger than $50/0.005/3600 \approx 2.8$ h. Hence, a leak detection level of 0.005 Nm could be met. Early Cassini flight data indicate that hydrazine is being consumed at a rate of about 1–1.5 g/day. This consumption rate is likely to decrease once the S/C gets farther away from the sun. Using a worst-case hydrazine consumption rate of 1.5 g/day, an upper bound on the per-axis angular momentum (due to thruster uncertainty) that is accumulated over 10 h is ≈0.05 Nms. It is about three orders of magnitude smaller than R_T (50 Nms). As such, $T^{\text{limit}} = 10$ h is a good choice for the cruise phase of the Cassini mission. The time threshold T^{limit} is changeable using the same command that is used to alter R_T. It is to be changed several times throughout the mission to reflect the changing torque detection levels already described (see also Fig. 4).

Simulation Results

The coded leak detection design was tested using the Cassini Flight Software Development Testbed. Attitude control actuators, e.g., thrusters, attitude determination sensors, and the S/C itself are represented by validated analytical models in this testbed. This testbed can simulate both the pulse-to-pulse and thruster-to-thruster variations, as well as disturbance torques due to a leaky thruster.

The leak detection monitor is designed to perform its function in many S/C scenarios: during a spiral sun search, while the spacecraft is in a quiescent state with its attitude controlled by either the thrusters or reaction wheels, while the S/C is being slewed about its Y axis (or Z axis) using either the thrusters or reaction wheels, and others. As such, its performance in all of these scenarios has

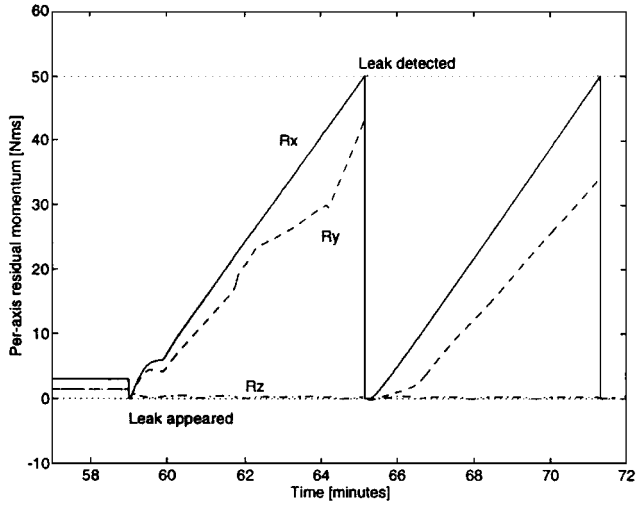

Fig. 6 Time histories of residual momenta.

to be evaluated. In each of these scenarios, test variants that represent combinations of the following selections must be generated and tested:

1) One of the eight prime thrusters ($Y_1 - Y_4$ and $Z_1 - Z_4$) is selected as the leaky thruster.

2) The leaky thruster is from either the A or B thruster branch.

3) Leakage levels may vary from 0.1–100% of the nominal thrust of the thrusters.

4) The time at which the leak occurred must be considered. For example, the leak might occur during the acceleration, coast, or deceleration phase of a spacecraft slew.

A multitude of test variants have to be generated and tested to provide a comprehensive validation of the performance of the error monitor design in all S/C scenarios. For brevity, only results obtained for a scenario in which the Z_1 thruster develops a 10% leak while the S/C is being slewed about the Y axis are given here.

With reference to Fig. 3, we see that a 10% leak in the Z_1 thruster will generate disturbance torques of −0.158 and +0.124 Nm about the S/C's X and Y axes, respectively. These torques will cause the X and Y components of $\boldsymbol{R}$ to grow with time (cf. Fig. 6). About 6 min (which is well below T^{limit}) later, $|R_x|$ first exceeded R_T, causing the X-axis error monitor to be triggered. In this particular simulation, we assume that the first corrective action initiated by the fault protection logic (the reseting of the controller unit of the thruster valve drive electronics) does not stop the leak (as shown in Fig. 6). Accordingly, both R_x and R_y will continue to grow with time after having been reset to zero. The next triggering of the error monitor will lead to the swapping of thruster branches, which stopped the leak.

Limitations of the Error Monitor Design

The current error monitor is not designed to detect a thruster leak if it occurs during any of the following S/C scenarios: 1) a ΔV is being performed by the main engine, 2) a ΔV is being performed by the four Z-facing thrusters, and 3) the S/C is being detumbled by the eight thrusters. Also, there is no requirement to detect the occurrence of a thruster leak that is of the following nature: 1) an intermittent leak, 2) a leak that is smaller than 0.1% of the nominal thrust of the thrusters, and 3) the simultaneous occurrence of two leaky thrusters.

Conclusions

A set of three model-based thruster leakage detection monitors has been designed, tested, and implemented in the flight software to protect Cassini against the occurrence of a thruster leak, a highly unlikely event. The computational effort involved in executing this set of monitors by the flight computer is moderate. With only two thresholds to select, this set of monitors could be easily managed by Mission Operations controllers. Simulation test results indicated that the design meets all of the requirements. In particular, the design can detect thruster leaks that are ≈0.1% of the thruster magnitude

and does so quickly before an unacceptable level of angular momentum is imparted on any S/C axis. The robustness of the design against knowledge uncertainties of various S/C parameters, as well as estimation erros of various S/C-derived variables, has also been confirmed via extensive simulations and early flight experience.

Appendix: Which Thruster Leaks?

One source of telemetry data that could be used to identify the leaky thruster is the time histories of the per-axis attitude control errors (which are denoted by e_i, $i = x$, y, and z axis). As indicated in Table A1, because a leaky Y_1 thruster generates both a positive and a negative torque about the X and Z axes, respectively, e_x and e_z will be stuck at $-\mathrm{db}_x$ and $+\mathrm{db}_z$, respectively (db_i is the attitude controller deadband for the S/C's ith axis). With no torque on the Y axis, e_y will fluctuate between $\pm\mathrm{db}_y$. Attitude controller error signatures of other leaky thrusters are tabulated in Table A1. By studying the time histories of these e_i components, we can both detect the presence of a leaky thruster and identify which thruster leaks.

Another source of telemetry data that could be used to detect the presence of a leaky thruster is the accumulated ontime's of the eight prime thrusters (T_j^{on}, where $j =$ thrusters Y_1–Y_4 and thrusters Z_1–Z_4). Specifically, the time rates of increase of these ontimes, T_j^{on}, will reveal the identity of the leaking thruster.

Table A1 Per-axis attitude control error signatures

Leaky thruster	Attitude control errors, mrad		
	X axis	Y axis	Z axis
Y_1	$-\mathrm{db}_x$	$\pm\mathrm{db}_y$	$+\mathrm{db}_z$
Y_2	$-\mathrm{db}_x$	$\pm\mathrm{db}_y$	$-\mathrm{db}_z$
Y_3	$+\mathrm{db}_x$	$\pm\mathrm{db}_y$	$+\mathrm{db}_z$
Y_4	$+\mathrm{db}_x$	$\pm\mathrm{db}_y$	$-\mathrm{db}_z$
Z_1	$+\mathrm{db}_x$	$-\mathrm{db}_y$	$\pm\mathrm{db}_z$
Z_2	$+\mathrm{db}_x$	$+\mathrm{db}_y$	$\pm\mathrm{db}_z$
Z_3	$-\mathrm{db}_x$	$+\mathrm{db}_y$	$\pm\mathrm{db}_z$
Z_4	$-\mathrm{db}_x$	$-\mathrm{db}_y$	$\pm\mathrm{db}_z$

Table A2 Signatures of $\dot{T}^{\mathrm{on}}$

Leaky thruster	Thruster ontime rates, s/s							
	Y_1	Y_2	Y_3	Y_4	Z_1	Z_2	Z_3	Z_4
Y_1	0	r	0	r	r	r	0	0
Y_2	r	0	r	0	r	r	0	0
Y_3	0	r	0	r	0	0	r	r
Y_4	r	0	r	0	0	0	r	r
Z_1	0	0	0	0	0	r	$2r$	r
Z_2	0	0	0	0	r	0	r	$2r$
Z_3	0	0	0	0	$2r$	r	0	r
Z_4	0	0	0	0	r	$2r$	r	0

Consider the scenario when the Z_1 thruster leaks. A negative and positive external torque will soon appear on the S/C's X and Y axes, respectively. With this combination of external torques, the Z_3 thruster, which is located diagonally opposite the leaky Z_1 thruster, will be fired at a rate that is about double that of the other two Z thrusters (Z_2 and Z_4). This is because the Z_3 thruster must negate external torques that appeared on both the S/C's X and Y axes. On the other hand, the Z_1 thruster, which is leaking, will not be fired. Accordingly, if the rate of increase of the ontimes of the Z_2 and Z_4 thrusters is r, then the rate of increase of the ontime of the Z_3 thruster should be $2r$ and that for the Z_1 thruster is 0. Note the Z_1 row of Table A2. Without any external torque on the S/C's Z axis, none of the Y thrusters will be fired. Hence, the rates of increase of all of the Y thrusters' ontimes are negligible (accordingly, we place 0 in the Y_1–Y_4 columns of the Z_1 row in Table A2). A complete mapping between the leaky thruster and the corresponding thrusters' ontime rates is given in Table A2.

Acknowledgments

The research was carried out by the Jet Propulsion Laboratory (JPL), California Institute of Technology, and was sponsored by NASA. The author is indebted to M. J. Brown, his collegue at JPL, for performing numerous simulation test runs. The author is also grateful to T. Barber, R. Belenky, C. Bell, W. Breckenridge, G. M. Brown, J. Chodas, C. Jennings, S. Johnson, M. Lam, M. Leeds, G. Macala, A. Mark, S. Peer, R. Rasmussen, and D. Skulsky at JPL and K. Hilbert, formerly with JPL, for many helpful discussions. The methodology described has been reported to the Patent Counsel Office of JPL on June 1998 for potential patent application.

References

[1] Jaffe, L., and Herrell, L., "Cassini Huygens Science Instruments, Spacecraft, and Mission," *Journal of Spacecraft and Rockets*, Vol. 34, No. 4, 1997, pp. 509–521.

[2] Wong, E., and Breckenridge, W., "An Attitude Control Design for the Cassini Spacecraft," *Proceedings of the AIAA Guidance, Navigation, and Control Conference*, AIAA, Washington, DC, 1995, pp. 931–945.

[3] Lee, A., "Cassini Orbiter Functional Requirements Book: Accuracy Requirements and System Capabilities," CAS-3-170, Jet Propulsion Lab., Internal Document, JPL D-699-205, rev. D, California Inst. of Technology, Pasadena, CA, Nov. 1997.

[4] Walker, J., and Lee, A., "Cassini Orbiter Functional Requirements Book: Attitude and Articulation Control Subsystem," CAS-4-2007, Jet Propulsion Lab., Internal Document, JPL D-669-205, rev. F, California Inst. of Technology, Pasadena, CA, Nov. 1997.

[5] Isermann, R., "Process Fault Detection Based on Modeling and Estimation Methods—A Survey," *Automatica*, Vol. 20, No. 4, 1984, pp. 387–404.

J. A. Martin
Associate Editor